Journal of Catalysis **205,** 123–134 (2002)
doi:10.1006/jcat.2001.3422, available online at http://www.idealibrary.com on IDEAL®

Chemical Transformations, Molecular Transport, and Kinetic Barriers in Creating the Chiral Phase of (*R*,*R*)-Tartaric Acid on Cu(110)

M. Ortega Lorenzo, V. Humblot, P. Murray,[2] C. J. Baddeley,[3] S. Haq, and R. Raval[1]

Leverhulme Centre for Innovative Catalysis and Surface Science Research Centre, Department of Chemistry, University of Liverpool, Liverpool L69 7ZD, United Kingdom

Received June 5, 2001; revised August 29, 2001; accepted August 29, 2001

Metal surfaces modified by chiral molecules have been shown to be effective heterogeneous catalysts for enantioselective reactions; however, their performance is found to be critically affected by modification conditions. Recently, model chirally modified surfaces created by the adsorption of the well-known chiral modifier, (*R*,*R*)-tartaric acid on a Cu(110) single crystal surface, have been shown to exhibit a variety of surface phases (Ortega Lorenzo, M., Haq, S., Bertrams, T., Murray, P., Raval, R., and Baddeley, C. J., *J. Phys. Chem. B* 103 (48), 10,661 (1999). Of these, only the low-coverage (4 0, 2 3) and (9 0, 1 2) phases are thought to be important for the enantioselective reaction. In this paper we report a detailed study of these two phases using the surface spectroscopic techniques of RAIRS, LEED, STM, and TPRS, and show that a remarkable dynamic interplay exists between them depending on adsorption temperature, coverage, and holding time. At low exposures, the conversion from the initially formed (4 0, 2 3) phase to the thermodynamically preferred (9 0, 1 2) phase is associated with a local chemical transformation from the monotartrate to the bitartrate form, accompanied by a change in the two-dimensional organization of the adsorbed modifier molecules which involves significant molecular mass transport and expansion in adsorption area. Time-dependent RAIRS data following this process show that it conforms to first-order kinetics and possesses a significant kinetic barrier of 73 ± 2 kJ mol^{-1}. Interestingly, increasing coverage of modifiers at the surface reverses the phase stabilities and causes reverse transformation of the (9 0, 1 2) bitartrate phase into the more densely packed monotartarte (4 0, 2 3) phase. Thermal evolution of the surface phases shows they are very robust and stable up to temperatures of >430 K, after which explosive decomposition of the molecule occurs in which intramolecular bonds break to release H_2, CO_2, and CO products into the gas phase. This work provides a fundamental insight into the delicate balances responsible for the creation or destruction of chiral phases at modified metal surfaces. © 2002 Elsevier Science

Key Words: **heterogeneous enantioselective catalysis; tartaric acid, Cu(110); chiral surfaces; scanning tunnelling microscopy; reflection adsorption infrared spectroscopy; temperature-programmed reaction spectroscopy.**

1. INTRODUCTION

Some of the most effective heterogeneous catalysts for enantioselective reactions have been produced by modifying a metal surface with chiral molecules and, subsequently, conducting the enantioselective reaction on the modified surface (2–6). Within this class of catalysts, one of the most intensively studied system is that in which metal (Ni, Co, Cu) catalysts have been modified by optically active acids, e.g., (*R*,*R*)-tartaric acid, to induce the asymmetric hydrogenation of β-ketoesters, e.g., methylacetoacetate, (Fig. 1), producing the *R*-enantiomer with an enantioselective excess (*e.e.*) of ~95% (6, 7). However, at present, the techniques of modification are imperfect, and the knowledge of the modified interface is insufficient to allow prediction of what the most successful systems would be. As a consequence, one of the major difficulties has been the attainment of reproducible reaction rates and optical yields, and there is general agreement that enantioselectivity is critically affected by the method of catalyst preparation and the nature of the modification procedure (8–12).

In order to provide a fundamental understanding of the various phenomena occurring on solid enantioselective catalyst surfaces, we have created model stereodirecting surfaces by the adsorption of the well-known chiral modifier, (*R*,*R*)-tartaric acid [(*R*,*R*)-TA], on a Cu(110) single-crystal surface (1). This work has clearly revealed that a variety of surface phases are created upon adsorption of a single molecular layer of (*R*,*R*)-TA on the Cu(110) metal surface (1, 13, 14), each possessing different local chemical and bonding characteristics and different two-dimensional organizational structures, depending on adsorption temperature, coverage, and holding time. Of these various phases, the ordered (9 0, 1 2) bitartrate phase is believed to be catalytically relevant and to provide important insights into the creation of the enantioselective site (1, 13), since it is the only phase capable of coadsorbing

[1] To whom correspondence should be addressed. Fax: 44 151 794 3589. E-mail: raval@liv.ac.uk.

[2] Present address: Pros Con, Rushbrooke Park, Cobh, Co. Cork, Ireland.

[3] Present address: Department of Chemistry, University of St. Andrews, Fife KY16 9ST, United Kingdom.

0021-9517/02 $35.00
© 2002 Elsevier Science
All rights reserved.

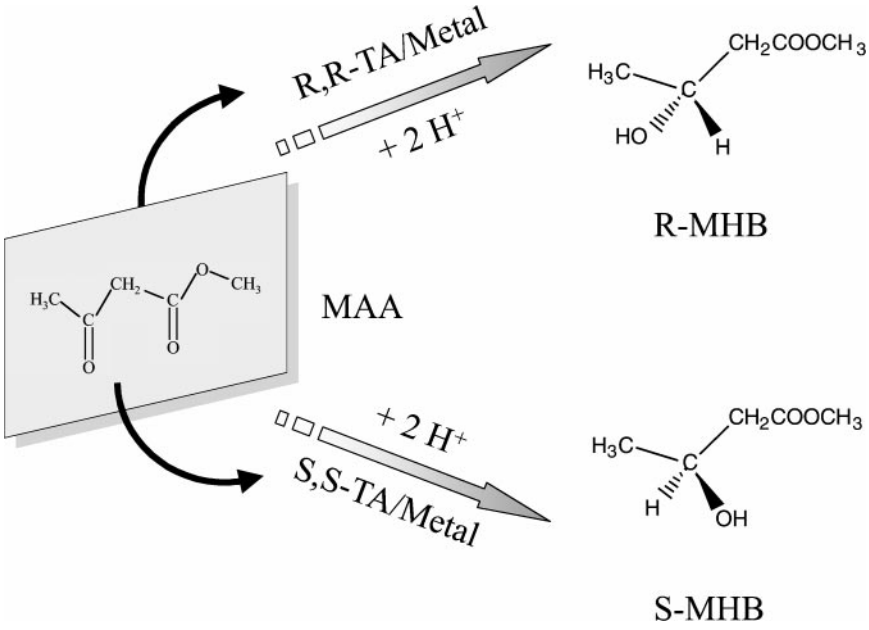

FIG. 1. Asymmetric hydrogenation of methylacetoacetate (MAA) to the enantiomer of the product molecule methyl-3-hydroxybutyrate (MHB).

the reactant, methylacetoacetate, within its structure. In this paper, we show that the creation of this phase is very condition dependent and involves a number of remarkable transformations in the interface. In order to trace the molecular details of this transformation, a number of surface science techniques such as reflection absorption infrared spectroscopy (RAIRS), low-energy electron diffraction (LEED), temperature-programmed reaction spectroscopy (TPRS), and scanning tunnelling microscopy (STM) were employed.

2. EXPERIMENTAL

RAIRS experiments were carried out in ultrahigh vacuum (UHV) chambers with a base pressure of $<1 \times 10^{-10}$ mbar, equipped with facilities for RAIRS, TPRS, LEED, Auger electron spectroscopy (AES), and sample cleaning. Detailed RAIRS spectra of each phase were obtained with the chamber interfaced with a Mattson 6020 FTIR spectrometer (data recorded with 4-cm^{-1} resolution with co-addition of 256 scans), while rapid RAIRS measurements following the kinetics of the transformation were carried out in a chamber interfaced with a Mattson 7020 spectrometer (data recorded with 4-cm^{-1} resolution with co-addition of 50 scans). Both FTIR spectrometers were equipped with liquid nitrogen-cooled HgCdTe detectors possessing a spectral range of 700–4000 cm^{-1}. All RAIRS spectra are displayed as ratios of sample single-beam spectra versus a reference background single beam of the clean Cu(110) crystal.

STM data were recorded in a third chamber, which accommodated an Omicron Vakuumphysik STM instrument along with LEED, AES, and sample cleaning facilities. All STM experiments were carried out with the sample at room temperature, and all images were acquired in constant current mode.

In each chamber, the Cu(110) crystal was cleaned by cycles of Ar^+ ion sputtering, flashing, and annealing to 750 K. The surface ordering and cleanliness were monitored by LEED and AES. (*R*,*R*)-tartaric acid (99%) was obtained from the Fluka Chemika Chemical Company and was used without further purification. The acid was contained in a small resistively heated glass tube, separated from the main vacuum chamber by a gate valve, and differentially pumped by a turbo molecular pump. Before sublimation, the (*R*,*R*)-tartaric acid (TA) was outgassed at ~330 K. The TA sample was then heated to ~370 K and exposed to the copper crystal. During sublimation the main chamber pressure was typically 2×10^{-9} mbar. Modifier coverage at the surface is given in terms of fractional monolayers (ML), quoted with respect to the number density of surface metal atoms. The adlayer unit mesh is given in standard matrix notation as

$$\begin{pmatrix} \mathbf{a}' \\ \mathbf{b}' \end{pmatrix} = \begin{pmatrix} G_{11} & G_{12} \\ G_{21} & G_{22} \end{pmatrix} \begin{pmatrix} \mathbf{a} \\ \mathbf{b} \end{pmatrix},$$

and quoted in the text as (G_{11} G_{12}, G_{21} G_{22}), where $\mathbf{a}'$ and $\mathbf{b}'$ are the overlayer net vectors; the underlying metal surface mesh is defined by $\mathbf{a}$, the unit vector along the ⟨1–10⟩; and $\mathbf{b}$, the unit vector along ⟨001⟩ directions.

TPRS spectra were collected between 273 and 573 K by heating the Cu(110) crystal while measuring the change in partial pressure for masses 2, 28, and 44 as a function of

sample temperature. Heating rates of ~2 K s^{-1} were used in TPRS experiments.

A CCD video camera interfaced to a computer was used for the digitization of the LEED patterns.

3. RESULTS AND DISCUSSION

3.1. Surface Phases Created at Low Exposures

Of the many phases created by (*R*,*R*)-tartaric acid on Cu(110) (1, 13, 14), only the low-coverage phases are able to be involved in the enantioselective hydrogenation of β-ketoesters, since these are the only ones that accommodate methylacetoacetate, the simplest reactant for this reaction, at the surface. At low exposures of (*R*,*R*)-TA to Cu(110), two distinct modifier adsorption structures are created that differ from each other in a number of ways. The spectroscopic data for these phases have been described in detail elsewhere (1), so their structures are only briefly described here. Each phase possesses a different two-dimensional organization at the surface giving rise to a (4 0, 2 3) adlayer in one case and a (9 0, 1 2) adlayer in the other. As a result, distinct LEED patterns and STM images are observed for each structure, which allow the detailed ordering and packing of the modifier molecules on the Cu(110) surface to be ascertained (Fig. 2). Furthermore, RAIRS data for each of these structures reveal another crucial difference, namely, that the (4 0, 2 3) phase is comprised of adsorbed monotartrate species, while the (9 0, 1 2) phase consists of the bitartrate species. A detailed analysis of surface spectroscopic data (1) reveals that the monotartrate species is bound to the surface via the deprotonated carboxylate group (Fig. 2b). In addition, the free COOH acid group is held away from the surface and is involved in considerable intermolecular H-bonding interactions with the alcohol groups of neighboring monotartrate species, leading to a strong tendency for island growth in this phase. RAIRS data from the (9 0, 1 2) phase show that it consists of the bitartrate species in which both acid groups are deprotonated, and the carboxylate functionalities thus created are bonded at the surface so that the modifier has a two-point bonding interaction with the metal and is held so that the C_2–C_3 bond is held almost parallel to the surface (Fig. 2a). Furthermore, the bitartrate (9 0, 1 2) phase possesses a remarkable quality in that the organization and growth directions of the adsorbed species are such that all symmetry planes of the underlying Cu(110) surface are annihilated, thus bestowing extended two-dimensional chirality onto the surface (13).

Although both structures described previously can be created with the same exposure of gases, the local modifier density within each structure is very different; the (4 0, 2 3) adlayer possesses a local coverage of 1/4 ML while the (9 0, 1 2) structure possesses a local coverage of 1/6 ML. This difference in local density has important consequences,

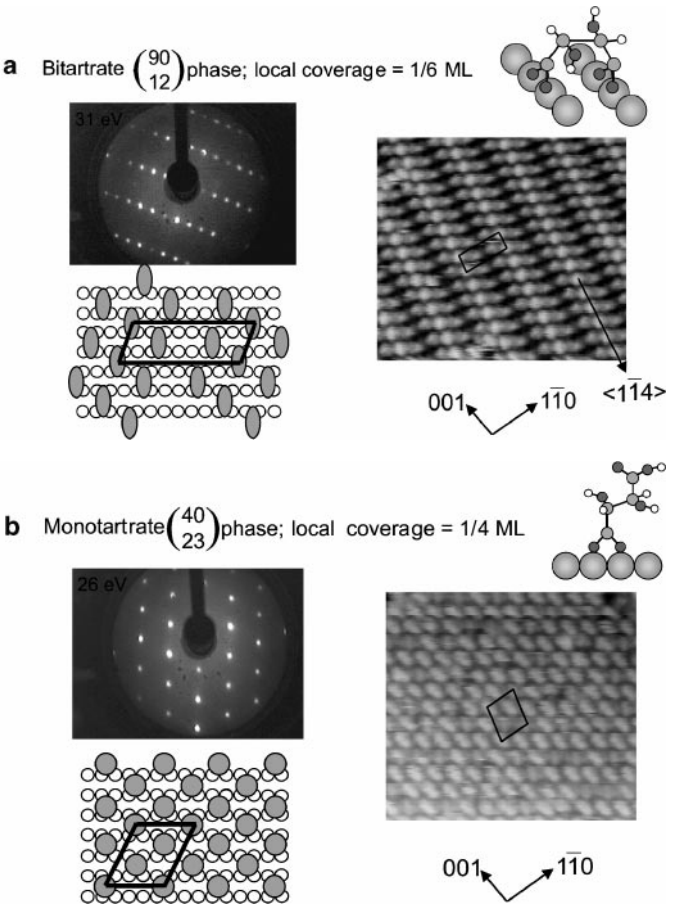

FIG. 2. (a) STM image (80 × 70 Å) (V_{tip}, −1.7 V; I_t, 1.18 nA) showing the (9 0, 1 2) bitartrate phase formed by (*R*,*R*)-tartaric acid adsorption on Cu(110) at ~350 K. A schematic diagram shows the position of the features observed in the STM image relative to the Cu(110) surface. (b) STM image (80 × 75 Å) (V_{tip}, −1.52 V; I_t, 1.25 nA) of the (4 0, 2 3) monotartrate phase formed by (*R*,*R*)-tartaric acid adsorbed on Cu(110) at 300 K. A schematic diagram of the adlayer is also shown.

with the extended chiral (9 0, 1 2) phase being the only one able to directly coadsorb the reactant methylacetoacetate within its structure and, thus, is strongly implicated in enantioselectivity.

3.2. Structural Interplay at Low Exposures

A number of factors determine whether the (4 0, 2 3) structure or the (9 0, 1 2) structure is formed and if there is interconversion between them. In order to facilitate discussion, the dynamic interplay between the existences of these two structures at low exposures of (*R*,*R*)-tartaric acid onto Cu(110) is shown in Fig. 3 as a function of adsorption temperature and coverage. From this it can be seen that the preference for the (4 0, 2 3) and the (9 0, 1 2) structures is critically controlled by the coverage. Turning first to the low-coverage situation, our experiments show that if adsorption is carried out at temperatures close to 300 K, only the

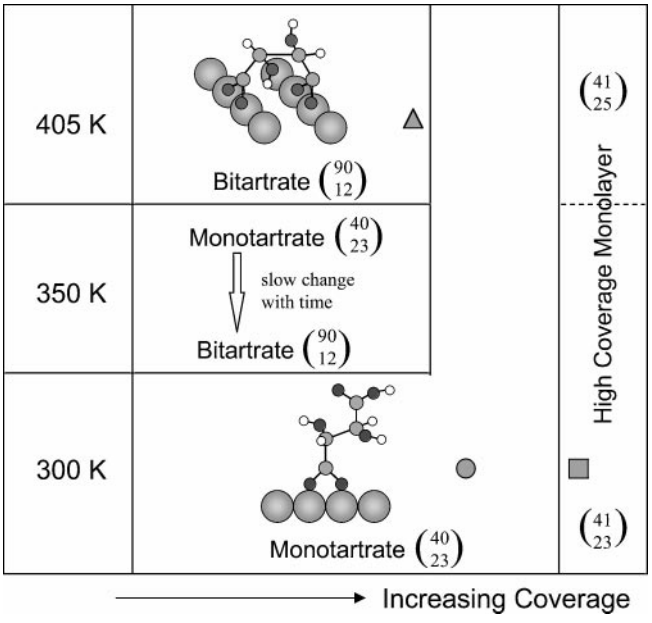

FIG. 3. Adsorption phase diagram showing the molecular nature and two-dimensional order adopted by (*R*,*R*)-tartaric acid molecules on a Cu(110) surface as a function of coverage, temperature, and time. (■, ●, and ▲ show points on the phase diagram at which TPRS experiments in Fig. 9 were carried out.)

monotartrate (4 0, 2 3) structure is formed and the bitartrate (9 0, 1 2) structure is never observed. However, at temperatures of above 405 K, the bitartrate (9 0, 1 2) structure forms immediately upon adsorption and is the preferred adsorbed form, being irreversibly retained when cooling down to 300 K. When adsorption is carried out at 350 K, the monotartrate (4 0, 2 3) structure is formed initially; but if the system is allowed to relax with time, a transformation of the monotartrate form to the bitartrate form is observed to take place. Figure 4 shows the RAIR spectra as a function of time after a small exposure of (*R*,*R*)-tartaric acid to the surface at 350 K. At $t = 0$ minute, the surface is covered in the low-coverage monotartrate phase. With increasing time, the feature at 1705 cm^{-1}, associated with the $\nu_{C=O}$ vibration of the monotartrate adsorbate, decreases in intensity until almost disappearing after 25 min, with the resulting spectra looking identical to those observed for the bitartrate phase (1). From this it would seem that in the early stages of adsorption at 300 K, (*R*,*R*)-tartaric acid adsorption is essentially frozen in the monotartrate conformation on the time scale of our experiments, while at 405 K and above, the molecules are able to relax almost immediately into the bitartrate conformation. Clearly, a kinetic barrier exists to the formation of the bitartrate (9 0, 1 2) form. Finally, we note that this transformation only occurs in the early stages of adsorption when small islands of the (4 0, 2 3) structure are present.

Our surface spectroscopic data reveal that a number of phenomena accompany the conversion of the monotartrate (4 0, 2 3) structure into the bitartarte (9 0, 1 2) structure. These various aspects are discussed in detail in the following.

3.2.1. Mass transport and area expansion. Time-elapsed RAIRS data (Fig. 4) clearly indicate that the conversion of the (4 0, 2 3) structure into the (9 0, 1 2) stucture involves a local chemical transformation in which the adsorbed monotartrate species deprotonate to form the bitartrate species. This time-dependent conversion of the phases is also seen in LEED experiments. However, it is STM data that dramatically illustrate the spatial implications of this transformation. Figure 5 shows STM data captured at 350 K, where the coexistence of the (4 0, 2 3) and the (9 0, 1 2) structures is observed. It can be seen from these data, that the (9 0, 1 2) structure emanates from the edges of the (4 0, 2 3) structure and flows out to expand onto the adjacent areas of the bare Cu(110) surface. The beginnings of this transformation are seen in the area labeled "b" where modifier molecules held within the (4 0, 2 3) islands. Areas labelled "a" are observed to have diffused away from their original position leading to "fraying" of the island edge. Areas marked "c" show that the modifier molecules issuing from the island self-assemble into the new structure with the (9 0, 1 2) repeat unit. The STM image in Fig. 5 also

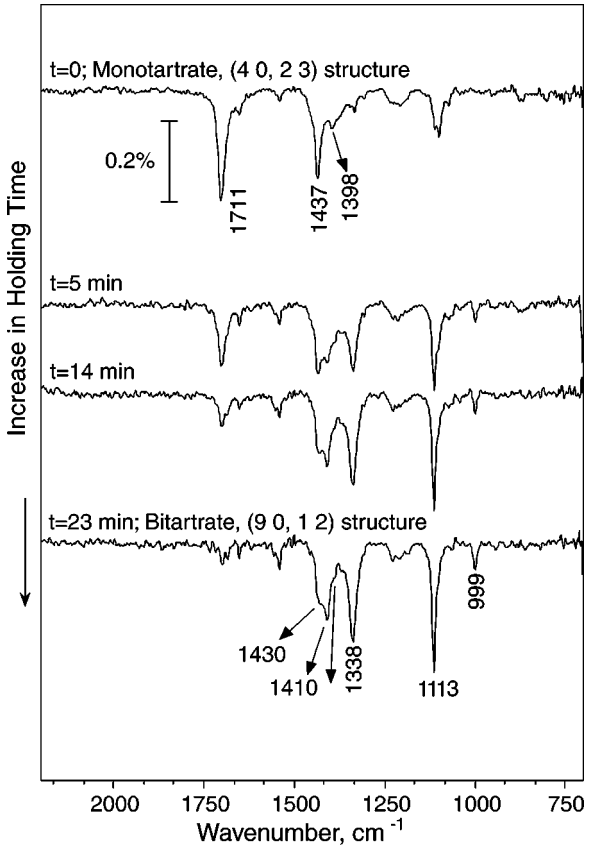

FIG. 4. RAIR spectra of (*R*,*R*)-tartaric acid on Cu(110) obtained as the sample is held at 350 K for increasing time intervals.

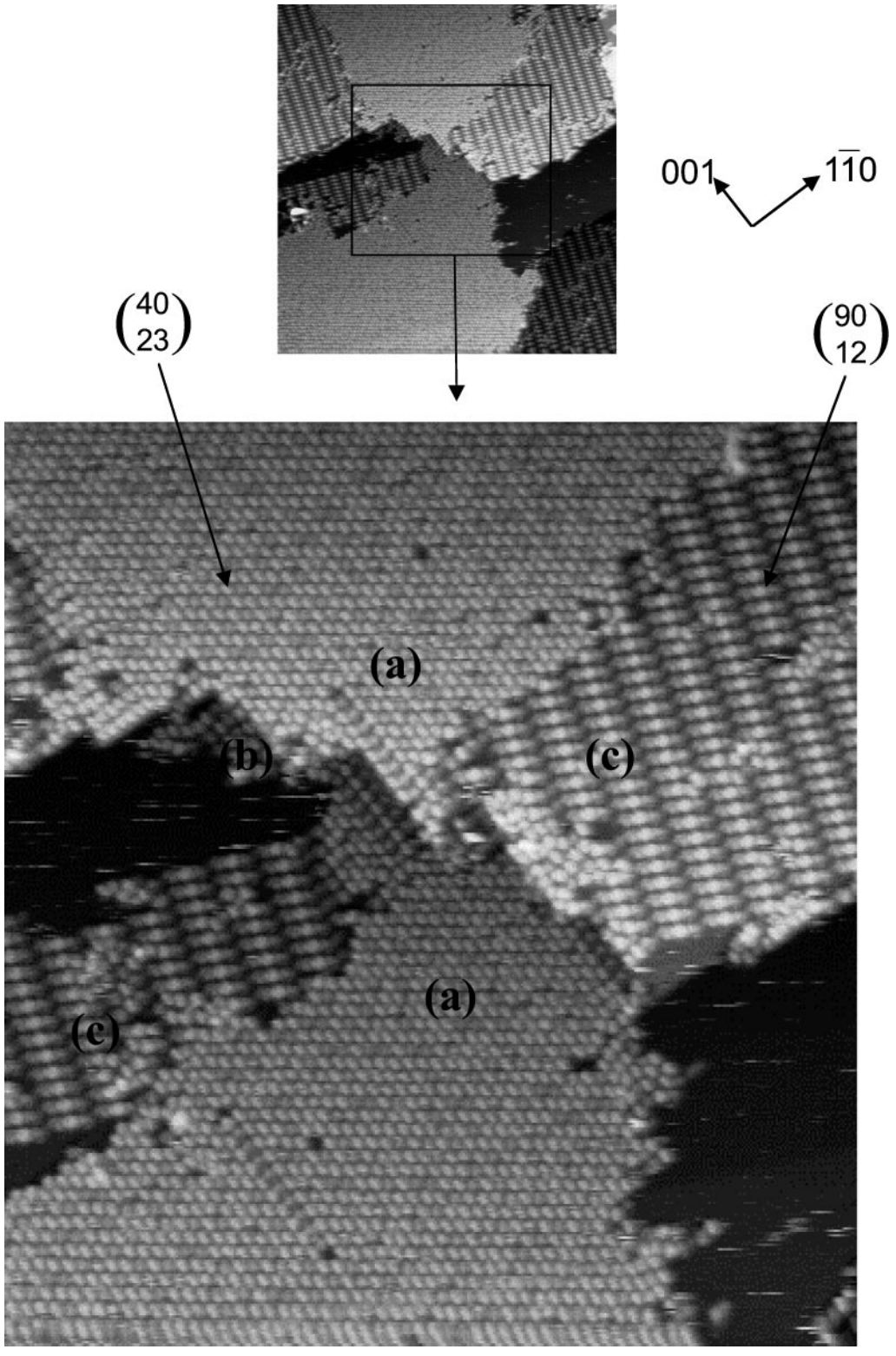

FIG. 5. STM images (500 × 500 Å) (V_{tip}, −1.52 V; I_t, 1.25 nA) and (300 × 300 Å) (V_{tip}, −1.52 V; I_t, 1.25 nA) of low-coverage phases of (*R*,*R*)-tartaric acid deposited on Cu(110) at 350 K, showing a mixture of (4 0, 2 3) (areas labeled a), and (9 0, 1 2) structures (areas labeled c). (b) Displays area where the transition is being initiated.

reveals that a large adsorbate transport occurs during the monotartrate/bitartrate conversion, which effectively leads to a significant expansion in the adsorption area as the local coverage is reduced from 1/4 ML in the (4 0, 2 3) structure to 1/6 ML in the (9 0, 1 2) structure. Mass transport and area expansion are more graphically illustrated in Fig. 6, where time-elapsed STM images tracking the evolution of the (9 0, 1 2) structure from the (4 0, 2 3) structure at 350 K are displayed, indicating that the original (4 0, 2 3) islands dissolve as adsorbed modifier molecules diffuse away to form the new structure, seemingly involving effective mass transport of the adsorbed modifier molecules across distances of 10's to 100's of Å across the metal surface. We note that it is not possible, on the basis of the STM data, to provide a detailed molecular view on exactly how this mass transport is achieved, i.e., whether individual adsorbates diffuse long distances (100's of Å) across the surface, or whether the boundary frontiers are advanced by local, short-range migrations of the adsorbates (<10 Å).

This area expansion now explains why the transformation can only occur in the early stages of adsorption when small islands of the (4 0, 2 3) structure are present, surrounded by areas of bare metal into which the expansion can proceed. If adsorption is continued until large islands of the (4 0, 2 3) structure are created, leaving little bare metal available for expansion, then conversion to the bitartrate form is suppressed even at high temperatures.

3.2.2. Kinetic barriers to creating the (9 0, 1 2) chiral phase. The time-dependent and temperature-dependent behaviors of the transformation of the (4 0, 2 3) structure into the (9 0, 1 2) structure suggest the presence of a kinetic barrier. In order to evaluate this barrier, time-dependent RAIRS experiments were carried out at a range of temperatures following the conversion of the monotartrate species found in the (4 0, 2 3) structure into the bitartrate structure that exists in the (9 0, 1 2) structure. The two species can be differentiated because RAIR spectra observed for the monotartrate adsorbate differ in a number of respects from those of the bitartrate phase, with the RAIR spectrum shown in Fig. 4a being representative of the former and that in Fig. 4d being representative of the latter. For example, the spectrum observed for the bitartrate form shows an almost complete absence of the $\nu_{C=O}$ band in the 1700-cm^{-1} wavenumber range in contrast to the strong signals observed in this region in the monotartrate phase. Changes are also observed for the carboxylate ν_{COO}^{sym} vibrational region where the single 1437-cm^{-1} band of the monotartrate is replaced by two closely spaced bands at 1430 and 1410 cm^{-1} for the bitartrate, attributed to either the coupling of the two identical COO^- oscillators on each molecule (15, 16) or to the presence of two inequivalent adsorption sites for the bidentate molecules on the surface (17). Additionally, changes are also observed in the 1338- and 1101-cm^{-1} bands, corresponding to the δ_{C-H} and ν_{C-OH} vibrations, respectively, which both increase in relative intensity and sharpen for the bitartrate phase compared to the monotartrate phase. This has been rationalized in terms of the geometry of the bitartrate species (Fig. 2a), in which the two carboxylate ends of the molecule are bonded to the surface, leaving the C_2–C_3 bond almost parallel to the surface. In this geometry, the C–OH bond is more directed toward the surface normal compared to the monotartrate species (Fig. 2b), while the C–H bond, which was almost vertical in the monotartrate species, adopts a new geometry more directed toward the surface parallel. Both these changes give rise to the observed strong dipole activity of the δ_{C-H} and ν_{C-OH} vibrations in the bitartate phase.

In order to carry out the kinetic measurements, the Cu(110) sample was subjected to low exposures of (*R*,*R*)-tartaric acid to create small islands of the (4 0, 2 3) phase, and RAIR spectra were collected every minute while the sample was held at a constant temperature. The phase change was best followed by mapping the decrease in the integrated intensity of the monotartrate $\nu_{C=O}$ vibration at the 1700-cm^{-1} band as a function of time (Fig. 7a). It can be seen that at 313 K, the integrated intensity of the 1700-cm^{-1} band hardly alters even after 60 min. In contrast, at 373 K, the intensity of the 1700-cm^{-1} band reduces to 20% of its initial value after only ~2 min. All the data conform well to the integrated first-order rate law (Fig. 7b), allowing the rate constant, k, to be measured at each temperature. An Arrhenius plot (Fig. 7c) then yields an activation energy, E_a, of 73 ± 2 kJ mol^{-1}. From this it is clear that the creation of the extended chiral (9 0, 1 2) phase is associated with a very significant kinetic barrier. The spectroscopic data presented in this paper allow some of the processes that contribute to this barrier to be qualitatively identified as follows. First, the local chemical conversion in which one monotartrate species is converted to a bitartarte species involves a second deprotonation event. As a comparison, the ΔG° value for the second deprotonation of TA molecules in solution to convert from the monotartrate form to the bitartrate form is only ~24.76 kJ mol^{-1} (18). Second, monotartrate molecules in the (4 0, 2 3) phase are involved in a network of H-bonding interactions within the structure. Therefore, the phase transformation necessarily involves a disruption of these interactions, which would entail its own activation barrier. That this effect is important is revealed by our experiments on the adsorption of the related molecule, succinic acid (HOOC–CH_2–CH_2–COOH) on Cu(110) (19). In contrast to the tartaric acid adsorption system, the doubly deprotonated bicarboxylate species is produced immediately upon adsorption of succinic acid on Cu(110) at 300 K, suggesting that a significant kinetic limitation to bitartrate formation must be attributed to the presence of the α-hydroxy groups and their involvement in strong intermolecular H-bonding interactions, which leads to the initial creation of the denser monotartrate phase.

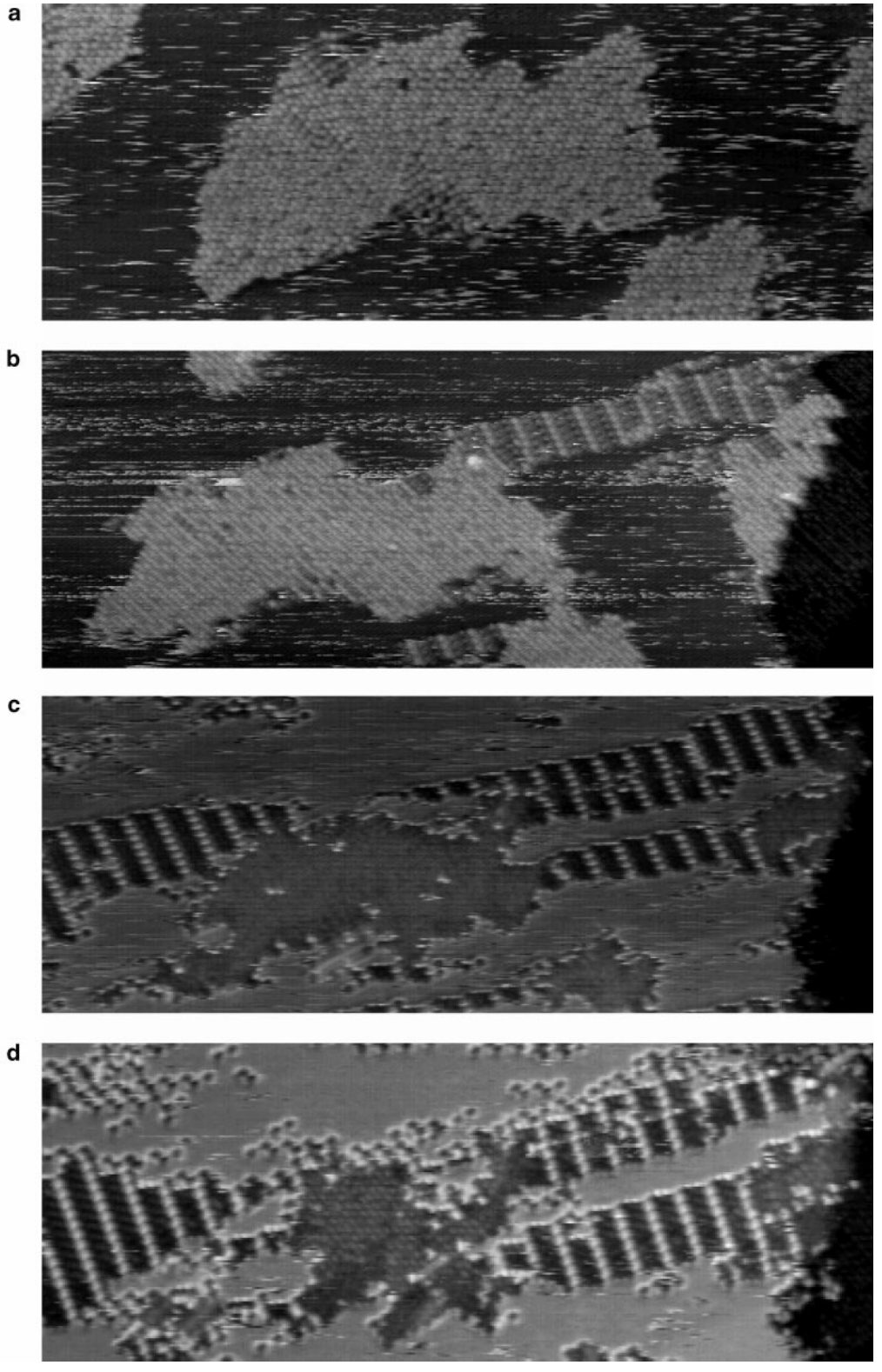

FIG. 6. STM images of a low coverage of (*R*,*R*)-tartaric acid deposited on Cu(110) at 350 K, showing the conversion of the (4 0, 2 3) structure to the (9 0, 1 2) when the system has been left to relax. Images (a), (b), (c), and (d) were recorded under the same conditions (70 × 430 Å) (V_{tip}, −1.08 V; I_t, 1.32 nA). It should be noted that all images are recorded for the same area of the surface.

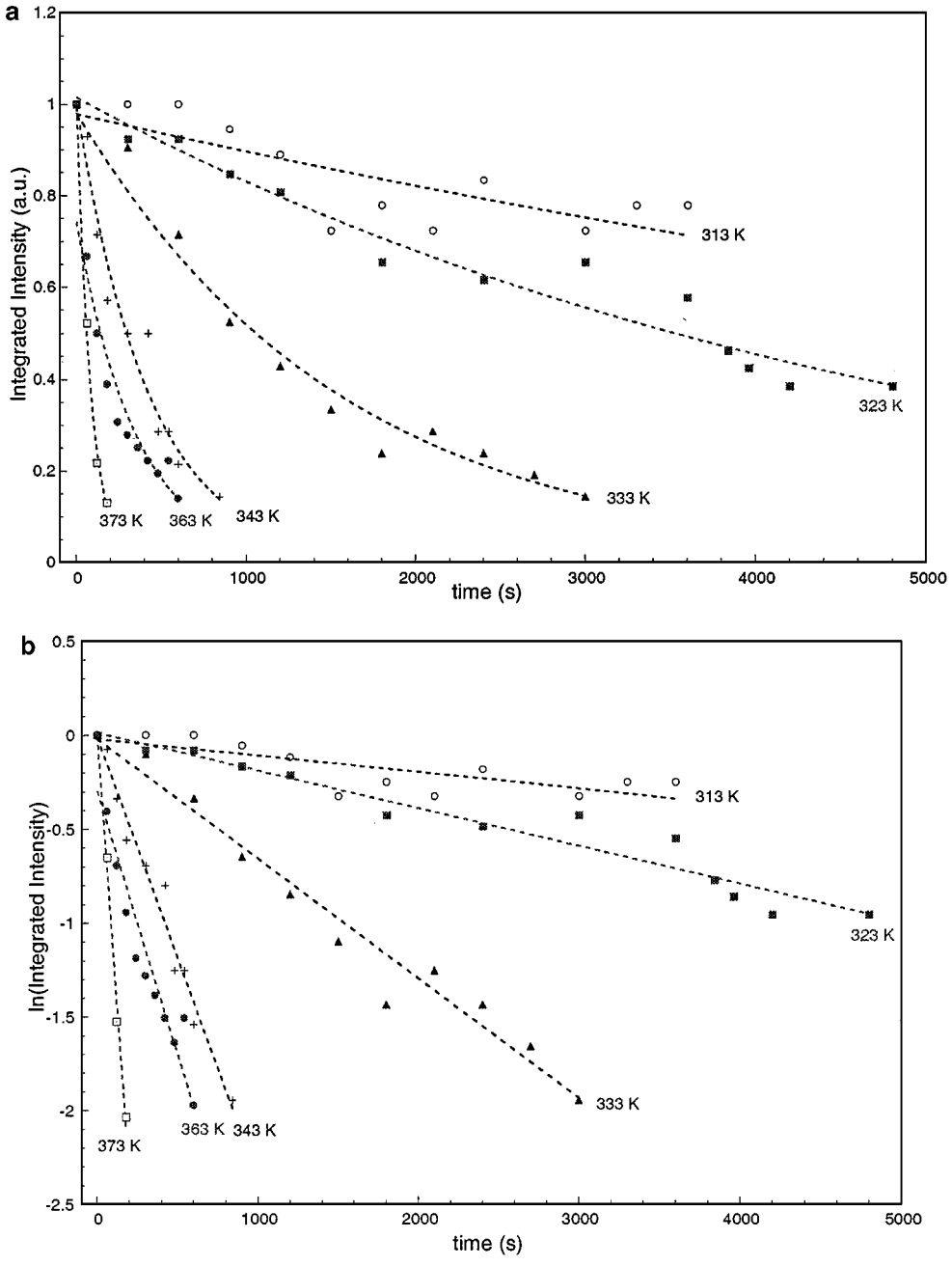

FIG. 7. Kinetic data obtained for the transition of the (4 0, 2 3) structures to the (9 0, 1 2) phases. (a) and (b) Decrease of the integrated intensity of the 1700-cm^{-1} band and natural logarithm of the integrated intensity of the 1700-cm^{-1} band plotted as a function of time for the following temperatures: ⊡, 373 K; ●, 363 K; +, 343 K; ▲, 333 K; ■, 323 K; ○, 313 K. (c) Linear of the Arrhenius equation ($\ln k = \ln A - E_a/RT$) obtained from the kinetic data shown in (a) and (b). Ln $A = 19.001$, $-E_a/R = -8813.9$ K^{-1} obtained from this plot.

In addition to the previously described factors arising from the local chemical transformation, other effects also have to be taken into account. Importantly, we have shown that conversion from the (4 0, 2 3) to the (9 0, 1 2) phase involves significant mass transport and diffusion of adsorbates at surfaces. Since the (*R*,*R*)-tartaric acid species is held strongly at the surface as seen by TPRS data (discussed later), the activation barrier of diffusion would be expected to be significant. Although diffusion barriers have not been mapped for related systems, it is anticipated that the activation barrier for diffusion for the tartaric acid/Cu(110) system would lie somewhere inbetween the activation barrier for the more strongly adsorbed O/W(110) systems, valued at 59 kJ mol^{-1}, and that for the more weakly CO/Ni(100) system valued at 20 kJ mol^{-1} (20). Additionally, from the STM images shown in Fig. 6, it can be appreciated that

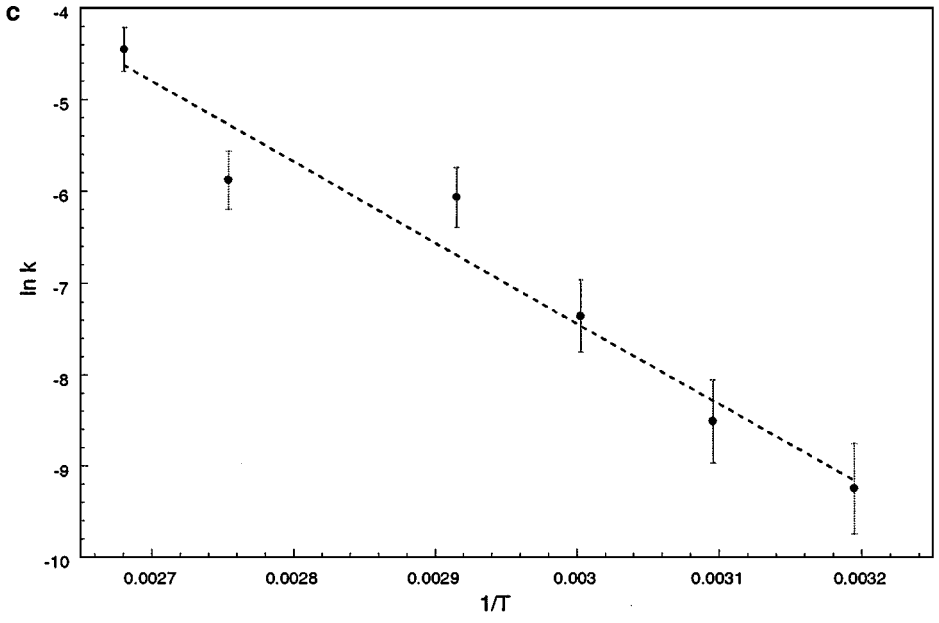

FIG. 7—*Continued*

the diffusion processes that lead to the (9 0, 1 2) area expansion are complicated and probably involve concerted and correlated movement of a number of bitartrate species in order to advance the frontiers of the (9 0, 1 2) islands. Finally, the possibility of local or large-scale reconstruction of the metal surface, of the type observed by Humblot *et al.* for (*R*,*R*)-TA/Ni(110) (21) must also be beared in mind, and could contribute to the high E_a of the monotartrate–bitartrate transformation.

3.3. Structural Interplay at High Exposure: Reversing the Phase Stabilities

From the previous discussion, it has been established that the monotartrate–bitartrate conversion effectively leads to a significant expansion in the adsorption area as the local coverage is reduced from 1/4 ML in the (4 0, 2 3) structure to 1/6 ML in the (9 0, 1 2) structure. This large increase in the adsorbed surface area also explains why the transformation only occurs in the early stages of adsorption when small islands of the (4 0, 2 3) structure are present, surrounded by areas of bare metal into which the expansion can proceed. A corollary of this effect is seen when the *reverse* transformation from the bitartrate form to the monotartrate form occurs when adsorption is continued to coverage beyond 1/6 ML. So, if adsorption is continued beyond a critical coverage so that large islands of the (4 0, 2 3) structure are created, leaving little bare metal available for expansion, then conversion to the bitartrate form is suppressed even at high temperatures. Interestingly, this is *not* due to an increased kinetic barrier to transformation, but rather to a reversal in phase stability. RAIRS data obtained at 405 K (Fig. 8) show that once the Cu(110) surface has been completely covered by the preferred low-coverage bitartarte (9 0, 1 2) structure, then an increased concentration of molecules at the surface is accommodated by the transformation of the bitartrate (9 0, 1 2) phase back to the

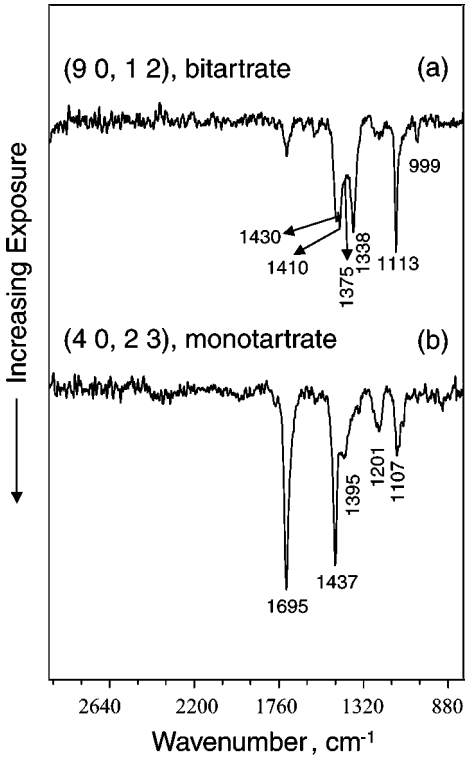

FIG. 8. RAIR spectra of (*R*,*R*)-tartaric acid on Cu(100) at 405 K obtained with increasing coverage showing the reverse transformation of the (9 0, 1 2) structure back to the (4 0, 2 3) structure.

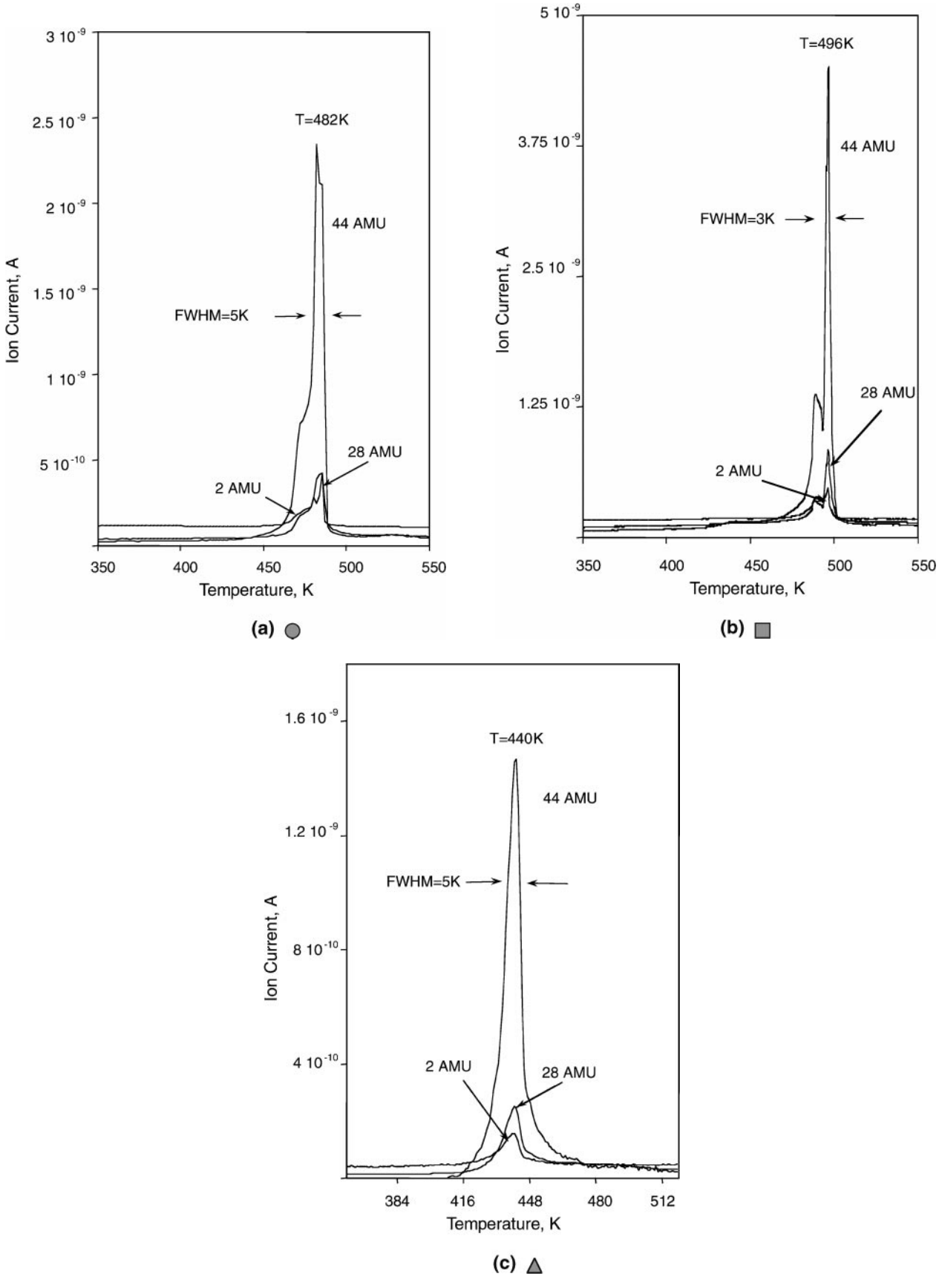

FIG. 9. TPRS obtained for: (a) ●, a low coverage monotartrate (4 0, 2 3) structure of (*R*,*R*)-tartaric acid adsorbed on Cu(110) at 300 K; (b) ■, a high coverage monotartrate monolayer (4 1, 2 3) structure of (*R*,*R*)-tartaric acid adsorbed on Cu(110) at 300 K; and (c) ▲, a low coverage bitartrate (9 0, 1 2) structure of (*R*,*R*)-tartaric acid adsorbed on Cu(110) at 405 K. Points at which these structures were formed are shown on the phase diagram (Fig. 3).

more densely packed monotartrate (4 0, 2 3) phase, which is then stable over the entire 300–450 K temperature range, as indicated in the adsorption phase diagram (Fig. 3). In order to effect this transformation, each bitartrate species has to pick up a hydrogen atom. Under UHV conditions and the temperatures of this experiment, Cu(110) is known not to hold a H reservoir at the surface; i.e., hydrogen created during the deprotonation processes, which lead to the mono- and the bi-tartrate species, recombinatively desorbs at these temperatures from the surface as H_2. Therefore, we propose that the hydrogen required to reverse the chemical transformation must be provided by the incoming bi-acid molecules, as

$$\underset{\text{adsorbed bitartrate}}{\text{OOCCH(OH)CH(OH)COO (a)}} + \underset{\text{incoming bi-acid}}{\text{HOOCCH(OH)CH(OH)COOH}} \longrightarrow \underset{\text{adsorbed monotartrate}}{2\ \text{OOCCH(OH)CH(OH)COOH (a)}}.$$

If exposure is increased beyond 1/4 ML (Fig. 3), then a new compressed structure is formed with a coverage of 0.3 ML in which monotartrate monomers and cyclic dimers coexist at the surface, ordered in a (4 1, 2 3) matrix in which substantial H-bonding interactions also exist. This structure has been described in detail elsewhere (1).

3.4. Thermal Evolution of Surface Phases

The thermal evolution of the various surface phases were monitored by heating the Cu(110) crystal at a constant temperature rate and monitoring the evolution products by mass spectrometry. The data from the low-coverage bitartrate (9 0, 1 2), the (4 0, 2 3) adlayer, and the highest coverage (4 1, 2 3) phase are shown in Fig. 9. In order to gauge the relative coverages, the phase diagram in Fig. 3 shows the points at which each of three adlayer structures was created. The first point that emerges from the thermal evolution of the (*R*,*R*)-TA/Cu(110) phases is that they are very robust and are stable up to temperatures of >430 K. A surprising fact that also arises is that the peak maximum temperature of product evolution increases as coverage is increased. This contradicts the thermodynamically preferred sequence for the filling of surface phases, where one would expect the preferred low-coverage phase to possess the highest heat of adsorption and, therefore, desorb at the highest temperature. However, inspection of the thermal evolution products shows that for all cases no desorption is observed at mass 75, the major ion of (*R*,*R*)-tartaric acid. This indicates that the data are not monitoring desorption of (*R*,*R*)-tartaric acid, but rather the products of surface decomposition of adsorbed TA molecules. In other words, reaction-limited desorption processes are observed suggesting that the molecule–metal interaction is so strong that intramolecular bonds break prior to metal–molecule bonds, with the decomposition products H_2, CO_2, and CO released in a sharp peak. This would explain why the bitartrate phase, which has the highest heat of adsorption and therefore the greatest perturbation (or activation) of the intramolecular bonds, decomposes at the lowest temperature of 440 K. In addition, for both the (4 0, 2 3) and the (4 1, 2 3) monotartrate phases, two desorption peaks are observed, with the second majority peak displaying a very narrow half-width of evolution (3–5 K). This behavior is very characteristic of explosive decompositions, first reported for formate and acetate species on Ni(110) (22, 23), and may be explained as follows: for both monotartrate structures, there is a retardation in the onset of decomposition of ~40 to 55 K compared to the bitartrate form, consistent with decreased activation of the molecular bonds as the surface interaction decreases. For a surface covered completely in either the (4 0, 2 3) or the (4 1, 2 3) structure, the lower coverage phases are inaccessible until this decomposition is initiated, creating enough free sites to trigger the relaxation of the structure to a lower coverage form. However, the lower reactivity of the high-coverage phase means that relaxation into the lower coverage structure occurs at a temperature that exceeds the thermal stability of that structure, triggering a concerted autocatalytic decomposition with explosive desorption of the decomposition products.

4. CONCLUSIONS

A detailed study of the remarkable dynamic interplay, depending on adsorption temperature, coverage, and holding time, between the existence of the bitartrate and monotartrate phases created by the well-known chiral modifier (*R*,*R*)-tartaric acid on Cu(110) has been described. The bitartrate (9 0, 1 2) phase is considered to be the most relevant for enantioselective catalysis and is found to be the most thermodynamically favorable stable structure at low coverages. However, adsorption at 300 K leads to the initial creation of the denser monotartrate (4 0, 2 3) phase. We show that a large kinetic barrier of 73 ± 2 kJ mol^{-1} exists for the transformation of the (4 0, 2 3) phase to the preferred bitartarte (9 0, 1 2) phase. As a result, the formation of the latter is very temperature dependent and time dependent. In addition, this transformation involves a large molecular transport and a significant expansion in adsorption area as the local coverage is reduced from 1/4 ML in the (4 0, 2 3) structure to 1/6 ML in the (9 0, 1 2) structure. Therefore, the transformation only occurs in the early stages of adsorption when small islands of the (4 0, 2 3) structure are present, flanked by areas of bare metal which are able to accommodate the increase in adsorption area. Finally, the relative stabilities of the monotartrate

and bitartrate phases alter dynamically with coverage, so that if adsorption is continued to high coverages, there is flipping of phase stability and the extra-modifier molecules are now accommodated by a reverse-phase transformation to the more densely packed monotartrate (4 0, 2 3) phase.

We note that the present study is confined to the modification of a Cu surface under UHV conditions, and so cannot be *directly* extended to the catalytically active system, which involves chirally modified Ni surfaces. However, certain general aspects reported here on the behavior of the chiral modifier may be important. For example, this work clearly shows that the nature of the adsorbed modifier phase at a metal surface is delicately affected by a number of factors, and very small changes in preparation conditions can trigger the creation of different structures, each expected to possess a very different enantioselective response. Such complicated behavior of the modified metal interface has now recently also been recorded on the catalytically more relevant Ni(110) surface (21) and provides some insights into the dramatic changes in *e.e.* observed in catalytic investigations when the reaction or modification conditions are changed. For example, the influence of the modification time (24–26), temperature (6, 25, 27–29), and modifier concentration (6, 25–26, 29–31) have all been shown to affect *e.e.* values. It is interesting to note that some of the best enantioselective TA/Ni catalysts have been created at a low modifier concentration of around 1/5 ML (12, 32, 33) with modification temperatures in excess of $T = 340$ K (12, 33). In addition, the delicate balances shown here to govern the creation of each phase may explain why a number of workers (7–12) report such difficulties in obtaining reproducible reaction rates and optical yields. In conclusion, it would seem that the interplay between a number of modifier surface phases must be beared in mind when optimizing catalyst preparation and reaction conditions.

ACKNOWLEDGMENTS

We are grateful to the EPSRC for equipment grants, postdoctoral fellowships to SH and PM, and a studentship to VH. We would also like to thank the Leverhulme Centre for Innovative Catalysis for a Ph.D. studentship for MOL.

REFERENCES

1. Ortega Lorenzo, M., Haq, S., Bertrams, T., Murray, P., Raval, R., and Baddeley, C. J., *J. Phys. Chem. B* **103**(48), 10,661 (1999).
2. Baiker, A., and Blaser, H. U., *in* "Handbook of Heterogeneous Catalysis" (G. H. Ertl, H. Knoezinger, and J. Weinheim, Eds), Vol. 5, p. 2422. VCH, New York, 1997.
3. Blaser, H. U., *Tetrahedron Asymmetry* **2**, 843 (1991).
4. Baiker, A., *Curr. Opinion Solid State Mater. Sci*. **3**, 86 (1998).
5. Tai, A., and Harada, T., *in* "Tailored Metal Catalysts" (Y. Iwasawa, Ed.), p. 265. Reidel, Dordrecht, 1986.
6. Izumi, Y., *Adv. Catal*. **32**, 215 (1983).
7. Harada, T., Haraki, K., Izumi, Y., Muraka, J., Ozaki, H., and Tai, A., "Proceedings, 6th International Congress on Catalysis, London, 1976" (G. C. Bond, P. B. Wells, and F. C. Tompkins, Eds.), p. 1024. The Chemical Society, London, 1977.
8. Hoek, A., Woerde, H. M., and Sachtler, W. M. H., "Proceedings, 7th International Congress on Catalysis, Tokyo, 1980" (T. Seiyama and K. Tanabe, Eds.), p. 376. Elsevier, Amsterdam, 1981.
9. Bostelaar, L. J., and Sachtler, W. M. H., *J. Mol. Catal*. **27**, 377 (1984).
10. Smith, G. V., and Musoiu, M., *J. Catal*. **60**, 184 (1979).
11. Wittmann, G., Bartok, G. B., Bartok, M., and Smith, G. V., *J. Mol. Catal*. **60**, 1 (1990).
12. Keane, M. A., and Webb, G., *J. Catal*. **136**, 1 (1992).
13. Ortega Lorenzo, M., Baddeley, C. J., Muryn, C., and Raval, R., *Nature* **404**, 376 (2000).
14. Raval, R., Baddeley, C. J., Haq, S., Louafi, S., Murray, P., Muryn, C., Ortega Lorenzo, M., and Williams, J., *Stud. Surf. Sci. Catal*. **122**, 11 (1999).
15. Srivastava, G. P., Mohan, S., and Jain, Y. S., *J. Raman Spectrosc*. **13**(1), 25 (1982).
16. Bhattacharjee, R., Jain, Y. S., Raghubanshi, G., and Bist, H. D., *J. Raman Spectrosc*. **19**, 51 (1988).
17. Bhattacharjee, R., Jain, Y. S., and Bist, H. D., *J. Raman Spectrosc*. **20**, 91 (1989).
18. Weast, R. C., Ed., "CRC Handbook of Chemistry and Physics," 54th edition. CRC Publishing, Cleveland, Ohio, 1973.
19. Ortega Lorenzo, M., Haq, S., Baddeley, C. J., and Raval, R., in preparation.
20. Adamson, A. W., "Physical Chemistry of Surfaces," 5th ed. Wiley–Interscience, New York.
21. Humblot, V., Haq, S., Muryn, C., Hofer, W., and Raval, R., *J. Am. Chem. Soc.*, to be published.
22. Falconer, J. L., and Madix, R. J., *Surf. Sci.* **46**, 473 (1974).
23. Madix, R. J., Falconer, J. L., and Suszko, A. M., *Surf. Sci.* **54**, 6 (1976).
24. Fish, M. J., and Ollis, D. F., *J. Catal*. **50**, 353 (1977).
25. Tatsumi, S., *Bull. Chem. Soc. Jpn*. **41**, 408 (1968).
26. Fu, L., Kung, H. H., and Sachtler, W. M. H., *J. Mol. Catal.* **42**, 29 (1987).
27. Hoek, A., and Sachtler, W. M. H., *J. Catal.* **58**, 276 (1979).
28. Fu, F., Kung, H. H., and Sachtler, W. M. H., *J. Mol. Catal*. **42**, 29 (1987).
29. Izumi, Y., Imaida, M., Fukawa, H., and Akabori, S., *Bull. Chem. Soc. Jpn*. **36**, 155 (1963).
30. Klabunovskii, E. I., Vedenyapin, A. A., Chankvetadze, B. G., and Areshidze, G. C., "Proceedings, 8th International Congress on Catalysis, Berlin, 1984," p. 543. Dechema, Frankfurt-am-Main, 1984.
31. Richards, D. R., Kung, H. H., and Sachtler, W. M. H., *J. Mol. Catal*. **36**, 329 (1986).
32. Webb, G., and Wells, P. B., *Catal. Today* **12**, 319 (1992).
33. Keane, M. A., *Langmuir* **13**, 41 (1997).